This information is current as of January 17, 2019.

Human Virus-Specific CD8+ CTL Clones Revert from CD45RO high to CD45RA high In Vivo: CD45RA high CD8+ T Cells Comprise Both Naive and Memory Cells

Mark R. Wills, Andrew J. Carmichael, Michael P. Weekes, Kim Mynard, Georgina Okecha, Ray Hicks and J. G. Patrick Sissons

---

References   This article **cites 32 articles**, 16 of which you can access for free at:
http://www.jimmunol.org/content/162/12/7080.full#ref-list-1

Why *The JI*? Submit online.

- **Rapid Reviews! 30 days*** from submission to initial decision

- **No Triage!** Every submission reviewed by practicing scientists

- **Fast Publication!** 4 weeks from acceptance to publication

*average

Human Virus-Specific CD8$^+$ CTL Clones Revert from CD45RO^{high} to CD45RA^{high} In Vivo: CD45RA^{high}CD8$^+$ T Cells Comprise Both Naive and Memory Cells[1]

Mark R. Wills,[2] Andrew J. Carmichael,[2] Michael P. Weekes,[2] Kim Mynard, Georgina Okecha, Ray Hicks, and J. G. Patrick Sissons

It has been generally believed that human CD8$^+$ memory cells are principally found within the CD45RO^{high} population. There are high frequencies of CD8$^+$ memory CTL specific for the human CMV tegument phosphoprotein pp65 in PBMC of long-term virus carriers; the large population of memory CTL specific for a given pp65 peptide contains individual CTL clones that have greatly expanded. In this study, we found high frequencies of pp65 peptide-specific memory CTL precursors in the CD45RO^{high}CD45RA$^-$ population, but also appreciable frequencies in the CD45RA^{high} subpopulation. Because the majority of CD8$^+$ T cells in PBMC are CD45RA^{high}, more of the total pp65-specific memory CTL pool is within the CD45RA^{high} than in the CD45RO^{high} compartment. Using clonotypic oligonucleotide probes to quantify the size of individual pp65-specific CTL clones in vivo, we found the CD45RA^{high} population contributed 6- to 10-fold more than the CD45RO^{high} population to the total virus-specific clone size in CD8$^+$ cells. During primary CMV infection, an individual virus-specific CTL clone was initially CD45RO^{high}, but after resolution of infection this clone was detected in both the CD45RO^{high} and the CD45RA^{high} populations. We conclude that CD45RA$^+$ human CD8$^+$ T cells do not solely comprise naive cells, but contain a very significant proportion of memory cells, which can revert from the CD45RO^{high} to CD45RA^{high} phenotype in vivo. *The Journal of Immunology,* 1999, 162: 7080–7087.

The leukocyte common Ag CD45 is a transmembrane tyrosine phosphatase that is expressed as isoforms of different m.w. as a result of differential splicing of three exons (A, B, and C) encoding part of the N-terminal extracellular domain. High m.w. isoforms of CD45 including exons A, B, and C or A and B are referred to as CD45RA; the low m.w. isoform that lacks exons A, B, and C is referred to as CD45RO (reviewed in Ref. 1). Analysis of human peripheral blood CD8$^+$ T cells by flow cytometry using mAbs that recognize either the high or low m.w. isoforms of CD45 shows subpopulations of cells that include CD45RA^{high} cells, CD45RO^{high} cells, and intermediate cells that coexpress CD45RA and CD45RO (2, 3). By regulating the extent of phosphorylation of key signaling molecules at the cell surface, the different isoforms of CD45 appear to regulate the responsiveness of T cells to diverse stimuli; CD45RO^{high}CD8$^+$ cells show greater proliferative responses to suboptimal anti-CD3 triggering compared with CD45RA^{high}CD8$^+$ cells (4).

In human cord blood, almost all CD8$^+$ T cells are CD45RA^{high}. With increasing age, the proportion of cells expressing CD45RO increases. Upon stimulation with Ag or mitogen in vitro, CD45RA^{high}CD8$^+$ T cells become activated and express CD45RO and down-regulate CD45RA (5). In human CD8$^+$ T cells, it has

been reported that the ability to respond to recall Ags mainly resides within the CD45RO$^+$ T cell population (6). It has therefore been proposed that CD45RA^{high}CD8$^+$ T cells constitute the naive T cell pool and that memory T cells express CD45RO, as has been proposed for CD4$^+$ T cells (7). However, there is evidence to suggest that for CD8$^+$ T cells this proposal may be an oversimplification. In adult PBMC, there is a subpopulation of CD45RA^{high}CD8$^+$ T cells that express high levels of CD11a (LFA-1); the size of this subpopulation increases with age, raising the possibility that these CD45RA^{high} cells may be primed cells (5). Indirect evidence from studies of the turnover of human T cell populations in vivo has suggested that CD45RO^{high} T cells may revert to CD45RA^{high} (8, 9), but these studies did not examine Ag-specific T cells. A recent study demonstrated that a substantial subset of CD8$^+$CD45RA$^+$ cells was stained with a EBV peptide-specific tetramer complex, suggesting that CD45RA is not a marker of naive T cells within the CD8$^+$ population (10).

To address the extent to which human Ag-experienced CD8$^+$ T cells revert from CD45RO^{high} to CD45RA^{high} in vivo, we studied the memory CD8$^+$ CTL response against human CMV (HCMV).[3] HCMV is a ubiquitous betaherpesvirus that infects between 60–90% of individuals depending on the population studied. Following primary HCMV infection, the virus persists lifelong in a latent state in cells of the myeloid lineage, under the control of the immune system, including CTL (11–16).

During T cell development in the thymus, the TCR $\alpha\beta$ heterodimer is generated by V(D)J gene recombination. Via the TCR, CD8$^+$ CTL recognize viral peptides presented by MHC class I molecules on the surface of infected cells. We have previously found high frequencies of memory CD8$^+$ CTL precursors (CTLp) specific for the HCMV tegument protein pp65 in the peripheral

Table I. *MHC class I tissue types, allele-specific pp65 peptides, TCR usage, and TCR Vβ n-D-n sequence for each donor in the study*

Donor	MHC Class I Type	pp65 Peptide (aa)	Class I Restriction	Predominant TCR Vβ Family Usage	TCR Vβ Sequence[a] Vβ	n-D-n	Jβ
OO1	A2 A2 B12(44) B27	p69 (495–503)	A2	13.1	tac	**caa act ggg aca ggg**	aac tat ggc
OO9	A2 A3 B7 B37 Cw6 Cw7	p56 (417–426)	B7	14	agt	**atc ggc ccg gcc c**	cg aac
OO5	A31 A33 B12(44) B35 Cw2	p17a (187–195)	B35	20	agt	**ccc acc ccc ggg agt agg**	act gaa gct
O15	A2 A3 B7 B7	p56 (417–426)	B7	6.4	tta	**cac gac agg gga tcg cgg**	act gaa gct
OO2	A9(24) A19(33) B7 B12(44) Cw5	p56 (417–426)	B7	14	agc	**gac ggg aca ggg gaa ggt ctg ggc**	tat ggc tac
102	A2 A28(69) B12(44) B37 Cw6 Cw7	p69 (495–503)	A2	ND			
104	A2 A2 B7 B7 Cw3 Cw7	p56 (417–426)	B7	6.4	tta	**atc ggc gag ggg aca ggg**	tgg cac gag
		p69 (495–503)	A2	ND			
		p31 (265–279)	B7	ND			

[a] The sequence of the clonotypic probes is indicated in bold. These sequences are available from EMBL under accession numbers AJ010878, AJ010889, AJ012537, AJ010890, AJ012538, and AJ012539.

blood of healthy virus carriers (16). We have recently analyzed the clonal composition of the memory CTL response to defined pp65 epitopes by generating multiple independent peptide-specific CTL clones and sequencing the hypervariable region of the TCR β-chain. In each healthy virus carrier, most of the CTL clones specific to a defined pp65 peptide use the same TCR β-chain at the level of nucleotide sequence, indicating that the large population of circulating peptide-specific memory CTL contains individual CTL clones that have greatly expanded in vivo (17). These clonal expansions are sufficiently large to permit direct molecular quantitation of the size of defined virus-specific CTL clones in PBMC.

In this study, we separated highly purified populations of CD45RA^{high} and CD45RO^{high} CD8^{+} T cells from PBMC of long-term HCMV carriers, and analyzed the distribution of functional pp65 peptide-specific memory CTLp and the distribution of defined peptide-specific CTL clonotypes. We also studied two patients through acute primary HCMV infection into long-term memory, and investigated the distribution of the pp65-specific memory CTL population as a whole, and of an individual pp65-specific CTL clone, in relation to changing CD45RA and CD45RO expression in CD8^{+} T cells.

In long-term virus carriers, we found that both the CD45RA^{high} and CD45RO^{high} populations contained peptide-specific CTLp; the same peptide-specific CTL clonotype was present in both CD45RA^{high} and CD45RO^{high} populations. During primary HCMV infection, we observed fresh ex vivo pp65-specific cytotoxicity associated with a large increase in CD45RO^{+}CD8^{+} T cells in PBMC. At subsequent time points, both the CD45RA^{high} and CD45RO^{high} populations contained peptide-specific CTLp, and a virus-specific CTL clone that was initially CD45RO^{high} subsequently became distributed in both the CD45RO^{high} and the CD45RA^{high} populations.

Materials and Methods

Donors

Five healthy HCMV-seropositive laboratory donors and two patients with primary HCMV were included in this study. All of the laboratory donors were HCMV seropositive, as determined by an IgG ELISA (Captia HCMV IgG immunoassay; Centocor, Malvern, PA). The patients with primary HCMV were confirmed by HCMV-specific IgM and subsequent seroconversion for HCMV-specific IgG (PHLS; Addenbrookes Hospital, Cambridge, U.K.). The MHC class I tissue type of each donor (Table I) was determined by serologic typing (Lymphotype ABC-120; Biotest, Dreieich, Germany).

Viruses and cell lines

HCMV AD169 (ATCC VR-538) was grown in GMO5387 fibroblasts (Coriell Cell Repositories, Camden, NJ) infected at a multiplicity of infection (moi) of 0.01. Whole infected cultures were harvested 5 days after 100%

cytopathic effect was evident, and were spun at 8000 rpm. Pellets were pooled, sonicated in an ice-cooled water sonication bath, aliquoted, and frozen at −70°C. Stocks were titered on 12-well plates of GMO5387s using 10-fold dilutions of virus; cytopathic effect was read after incubation for 10 days. Recombinant vaccinia viruses expressing the HCMV protein pp65 (vac pp65; gift of Dr. S. Riddel, Fred Hutchinson Cancer Research Centre, Seattle, WA), and a negative control expressing bacteriophage RNA polymerase T7 (vac T7) were grown in BHK cells infected at an moi of 0.1. After 48–72 h, the infected cells were harvested and subjected to three rounds of freeze-thaw, followed by sonication. The cell debris was removed by centrifugation, and supernatant-containing virus was aliquoted and stored at −70°C. A sample was subsequently titered on Vero cells; titers were normally between 1.5 and 10×10^7 plaque-forming units/ml.

Peptides based on the lower matrix protein pp65

Minimal peptides corresponding to proposed MHC-restricted epitopes of HCMV pp65 were synthesized and purified (>95%) by HPLC (Affiniti Research Products (Exeter, U.K.) (16, 17). All peptides were dissolved in RPMI 1640 at 200 μg/ml and frozen in small aliquots at −70°C.

mAbs and surface phenotyping

PBMC were prepared from fresh heparinized venous blood samples by Ficoll-Hypaque (Lymphoprep; Nyegaard, Oslo, Norway) density-gradient centrifugation. The surface phenotype of fresh PBMC and cells purified by cell sorting was determined by flow cytometry. mAbs conjugated with FITC, PE, or peridinin chlorophyll protein (PerCP) used were anti-CD4 FITC (Leu3a), anti-CD8 FITC/PE/PerCP (Leu2a), anti-CD16 FITC (Leu11a), anti-CD19 FITC (SJ25C1), anti-CD45RA FITC (Leu18), anti-CD45RO PE (UCHL-1), anti-CD56 PE (Leu19). The proportion of cells using specific TCR Vβ-chains was determined by three-color immunofluorescence using a panel of TCR-specific FITC-conjugated mAbs (the panel included: Vβ 1, 2, 3, 5.1, 5.2, 6.7, 7, 8.1, 11, 12, 13.6, 14, 16, 17, 19, 20, 21.3, and 22 (Coulter, Palo Alto, CA); Vβ 13.1/13.3 and Vα2 (Serotech)) with PE-conjugated anti-CD8 and PerCP-conjugated CD3. Samples were analyzed on a FACSort flow cytometer (Becton Dickinson, Oxford, U.K.) and using WinMDI software (Joseph Trotter, Scripps, http://facs.scripps.edu).

Preparation of cell populations

Total CD8^{+}, CD8^{+}CD45RO^{high}, and CD8^{+}CD45RA^{high} cells were prepared from PBMC using negative cell sorting to minimize any effects of ligation of CD8, CD45RA, or CD45RO on the cell surface. It is not possible to purify intermediate CD45RA^{+}RO^{+} cells by negative selection. PBMC were stained with FITC-conjugated anti-CD4, anti-CD19, anti-CD16, and anti-CD56 mAbs (to remove CD4^{+} T cells, B cells, and NK cells, respectively) and sorted for nonstained cells using a FACSVantage cell sorter (Becton Dickinson). CD8^{+}CD45RO^{high} cells were isolated by staining another aliquot of PBMC with anti-CD4, anti-CD19, anti-CD16, anti-CD56, and anti-CD45RA, and sorting for nonstained cells. CD8^{+}CD45RA^{high} cells were isolated by staining another aliquot of PBMC with anti-CD4, anti-CD19, anti-CD16, anti-CD56, and anti-CD45RO, and sorting for unstained cells. The purity of the CD45RA^{high} cells was >99% (CD45RO^{high} cell contamination 0.1–0.65%); the purity of the CD45RO^{high} cells was >99% (CD45RA high cell contamination 0.1–0.27%) (Fig. 1, *C* and *F*).

Generation of HCMV-specific CTL in limiting dilution assays (LDA)

Replicate microcultures ($n = 27$) of purified CD8⁺ T cell populations were set up in 96-well round-bottom plates in which the number of responder T cells per well was progressively reduced over an appropriate range of dilutions in RPMI 1640 supplemented with 10% human AB serum (HCMV seronegative; Blood Transfusion Service, Addenbrookes Hospital, Cambridge, U.K.), 2 mM L-glutamine, 10^5 IU/L penicillin, and 100 mg/L streptomycin (referred to as RPMI-HuAB). As stimulator cells, autologous PBMC were pulsed for 1 h with HCMV (moi 0.01), irradiated (2400 rad), and added at 5×10^4 cells/well. Although HCMV does not appear to establish a productive infection of unstimulated PBMC, exogenous pp65 protein is able to enter the MHC class I processing pathway (15) for stimulation of pp65-specific CD8⁺ T cells. The medium was further supplemented with human rIL-2 to give a final concentration of 5 IU/ml. LDA cultures were incubated at 37°C in 5% CO₂ and refed with RPMI-HuAB supplemented with 5 IU/ml IL-2 on days 5 and 10. On day 14, using split-well analysis, the cells in each individual well were resuspended and divided into aliquots that were assayed simultaneously for cytotoxicity against radiolabeled target cells in 4-h ⁵¹Cr release assays. Target cells comprised 4×10^3 cells/well autologous and MHC-mismatched lymphoblastoid B cell lines that were pulsed or unpulsed with pp65 peptide (40 μg/ml) for 1 h, or infected for 18 h with vac pp65 or control vac T7 (moi = 10). Target cells were washed three times and counted before use in chromium release assays. The LDA results were analyzed as described previously (16).

PCR amplification of TCR Vβ regions

Total RNA was extracted from $1–10 \times 10^5$ cells using an RNA extraction kit (Qiagen, West Sussex, U.K.). First strand cDNA was reverse transcribed with an oligo(dT) primer and avian myeloblastosis virus reverse transcriptase using a reverse-transcription kit (Promega, Madison, WI), according to the manufacturer's instructions. PCR was performed using a panel of 36 TCR Vβ family-specific primers (17) together with the corresponding C region-specific primer (synthesized by Genosys Biotechnologies, Cambridge, U.K.). Each reaction was conducted in a total volume of 50 μl containing 1 mM of each dNTP (Boehringer Mannheim, Indianapolis, IN), 3.75 mM MgCl₂, each primer at a final concentration of 1 mM, and 1 U of *Taq* polymerase (Promega), in buffer supplied by the manufacturer. A total of 2 μl of cDNA was used for PCR amplification in each case. The reaction was overlaid with mineral oil, and amplification was performed for 45 cycles of PCR. Conditions were 1-min denaturation at 94°C, 30 s of annealing at 60°C, and 30 s of extension at 72°C on a DNA thermal cycler (Perkin-Elmer Cetus 9600 Instruments, Norwalk, CT). A total of 45 μl of each PCR product was separated on a 1.3% agarose gel. Expression of Vβ genes was considered positive where an approximately 300–400 nt rearranged band could be visualized with ethidium bromide staining.

Quantitative clonotypic analysis

We previously generated peptide-specific CTL clones in vitro and sequenced the TCR β-chain (17). To quantify a defined peptide-specific CTL clone in PBMC by molecular assay, we designed a complementary oligonucleotide 15–20 nt long based on the TCR β-chain hypervariable n-D-n region of that immunodominant CTL clone (referred to as the clonotypic probe (Table I)). We also designed a conserved TCR C region probe to quantify total amplified TCR sequences. Vβ family-specific PCR was performed in duplicate on cDNA from total CD8⁺, CD8⁺CD45RA^high, and CD8⁺CD45RO^high cells from each donor. PCR products were also produced from the defined peptide-specific CTL clone (positive control) and from a mixed population of PBMC derived from four HCMV-seronegative donors (negative control). The duplicate PCR samples were separated on a 1.3% agarose gel, and the DNA was transferred onto a filter (Bio-Rad, Richmond, CA) using standard techniques in blotting buffer (0.6 M NaOH, 0.2 M NaCl) overnight. Filters were washed in 2× SSC and baked at 80°C for 30 min. Filters were prehybridized in 15 ml of 7% SDS, 0.25 M Na₂HPO₄ for 1 h at 10–15°C below Tm of the oligonucleotide probe. The oligonucleotide probes were end labeled with [α-³²P]dATP using T4 polynucleotide kinase; unincorporated label was separated from the probe using a G-25 Sephadex spin column (Amersham, Arlington Heights, IL). Filters were first hybridized with the clonotypic probe overnight at 10–15°C below the Tm of the clonotypic probe in hybridization buffer (7% SDS, 0.25 M Na₂HPO₄, 10% polyethelyne glycol 8000). After hybridization, the filters were washed three times (5% SDS, 20 mM Na₂HPO₄) for 15 min each. Binding of the probe was imaged and quantitated using a phosphor imager (Beckman, Fullerton, CA); the filters were also exposed to x-ray film. Bound clonotypic probe was removed from the filters by soaking in 0.4 M NaOH for 30 min, followed by one wash in 2× SSC. The

filter was then rehybridized with the TCR β-chain C region probe (AGATCTCTGCTTCTGATG) following the same protocol as for the clonotypic probe. In each experiment, it was possible to correct for differences in radioactive labeling and binding of the clonotypic and C region probes by measuring the radioactivity of each probe bound to the positive control sample as a reference standard (TCR β-chain sequences amplified from the biologically derived CTL clone contain the unique hypervariable n-D-n region and C region in equal amounts). The proportion of clonotype sequence within the total amplified TCR Vβ sequence for a given population of CD8⁺ cells was calculated as: test sample cpm (probed with clonotypic probe)/test sample cpm (probed with constant probe) × 100; positive control cpm (probed with clonotypic probe)/positive control cpm (probed with constant probe).

Results

In long-term healthy HCMV carriers, many of the pp65 peptide-specific CD8⁺ CTLp in PBMC are CD45RA^high

CD8⁺ T cells purified from PBMC of HCMV carriers by negative cell sorting were a mixture of CD45RA^high, CD45RO^high, and CD45RA⁺RO⁺ intermediates (Fig. 1A). Because CD8⁺CD45RA^high and CD8⁺CD45RO^high T cells are mutually exclusive populations, high purity CD8⁺CD45RA^high cells were obtained by sorting, using staining with anti-CD45RO and collecting negative cells (Fig. 1C); high purity CD8⁺CD45RO^high cells were obtained using staining with anti-CD45RA and collecting the negative cells (Fig. 1E). Each of the populations was stimulated in LDA with autologous irradiated HCMV-infected PBMC. Ag-specific cytotoxicity was assessed using target cells that expressed whole pp65 (vaccinia recombinant) and target cells that were pulsed with the immunodominant pp65 peptide appropriate for donor HLA type (Table I). In five long-term HCMV carriers, the CD8⁺ cell population as a whole contained high frequencies of pp65-specific CTLp (Fig. 1B; Table II). Both the CD8⁺CD45RA^high and CD8⁺CD45RO^high subpopulations contained pp65-specific CTLp, including CTLp specific to the same immunodominant pp65 peptide (Fig. 1, *D and F*; Table II).

In healthy HCMV carriers, CD8⁺ T cells in PBMC contained a higher percentage of CD45RA^high cells than CD45RO^high cells. In each HCMV carrier, the contribution of CD45RA^high and CD45RO^high cells to the total pool of pp65 peptide-specific memory cells in PBMC was determined by multiplying the peptide-specific CTLp frequencies within each T cell subpopulation by the percentage of CD45RA^high or CD45RO^high cells within CD8⁺ T cells in PBMC (Table II). In two healthy HCMV carriers (001 and 009), 10-fold more of the pp65 peptide-specific CTLp in PBMC were CD45RA^high than were CD45RO^high CD45RA⁻; in two other HCMV carriers (005 and 002), equivalent numbers of the pp65 peptide-specific CTLp in PBMC were CD45RA^high and CD45RO^high.

Large clone sizes of peptide-specific CTL clonotypes are present in CD45RA^high cells in long-term HCMV carriers

In each HCMV carrier, most of the independently derived pp65 peptide-specific CTL clones use the same TCR β-chain at the level of nucleotide sequence, indicating a high degree of clonal focusing (17). To quantify an individual peptide-specific CTL clone, we designed an oligonucleotide probe complementary to the hypervariable β-chain sequence of the CTL clone (Table I). In order first to determine the relationship between the amount of clonotypic DNA and the amount of bound radiolabeled probe in the blotting assay (see *Materials and Methods*), cDNA from a biological pp65 peptide-specific CTL clone was PCR amplified and added in increasing amounts to TCRs derived from a pool of cDNA from PBMC of four HCMV-seronegative donors. Each of the mixtures of TCR DNAs was probed first with the clonotypic probe (Fig. 2B) and, after stripping the filter, with the C region probe that binds to all TCR β-chain DNA sequences (Fig. 2C). The results show a
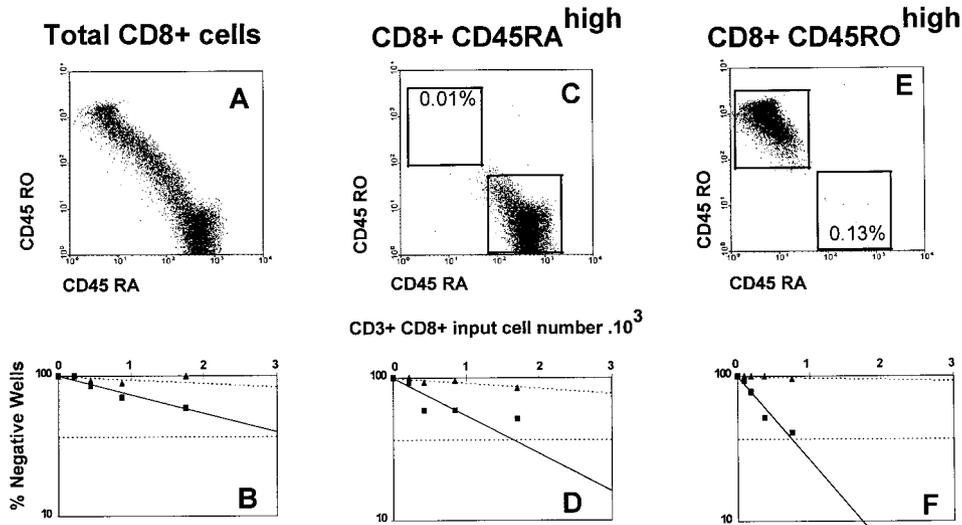
FIGURE 1. Separation of total CD8$^+$, CD8$^+$CD45RA^{high}, and CD8$^+$CD45RO^{high} T cells from PBMC by negative cell sorting and quantitation of pp65-specific CTLp frequencies within each population by LDA. Total CD8$^+$ cells were enriched from PBMC of donor 001 by staining with mAbs to CD4, CD16, CD19, and CD56 and sorting for negative cells. CD45RA^{high} cells were derived as for total CD8 cells with the addition of a mAb to CD45RO-PE and sorting for negative cells. CD45RO^{high} cells were derived as for total CD8 cells with the addition of a mAb to CD45RA-FITC and sorting for negative cells. *A*, *C*, and *E*, Aliquots of all sorted cells were restained with CD8-PerCP, CD45RA-FITC, and CD45RO-PE and gated on CD8$^+$ cells to assess the sorting purity. *B*, *D*, and *F*, All three populations were stimulated with autologous PBMC pulsed with HCMV, and CTLp frequencies were determined by LDA against target cells expressing vaccinia pp65 (■) and as a control vaccinia T7 (▲).

close correlation between the actual amount of clonotypic sequence added into the test samples and the experimentally derived values using clonotypic probing: the relationship is linear over a wide range (Fig. 2*D*) that includes the experimental values observed in subsequent experiments (Table III). The technique has the sensitivity to detect approximately 1% clonotype sequence against the background of 99% different n-D-n sequences within the corresponding Vβ family.

We used this probing technique to quantify the size of individual CTL clones in CD8$^+$ T cell populations purified directly from PBMC

of long-term HCMV carriers. We found that in a given carrier, the same pp65-specific CTL clonotype could be detected in both the CD45RA^{high} and CD45RO^{high} CD8$^+$ T cells. In some subjects, the clonotype constituted one-half of all of the TCR sequences in the relevant Vβ^+ population of CD8$^+$ cells (Fig. 3, Table III). The absolute clone sizes of individual peptide-specific CTL clones in the total CD8$^+$ population were very large, up to 0.8% of CD8$^+$ PBMC. In all donors tested, we found that the CD45RA^{high} population contributed 6- to 10-fold more than the CD45RO^{high} population to the total clone size in CD8$^+$ PBMC (Table III).

Table II. *Quantitation of pp65 peptide-specific CTLp in total CD8$^+$ T cell population and in the CD45RA^{high} and CD45RO^{high} CD8$^+$ subpopulations using LDA*

Donor (peptide/class I restriction)	T Cell Population	CTLp Frequencies per 10^6 Input Cells in Each Population by Target Cell Type			% of Cells in CD8$^+$ PBMC by Flow Cytometry	Contribution to the Peptide-Specific CTLp Frequencies in 10^6 CD8$^+$ PBMC[a]
		Vaccinia pp65	Vaccinia T7	pp65 peptide		
OO1 (p69/A2)	Total CD8	270	60	630	100	**630**
	CD45RO^{high}	1340	30	1140	3.7	**40**
	CD45RA^{high}	560	90	610	74	**450**
OO9 (p56/B7)	Total CD8	1830	20	900	100	**900**
	CD45RO^{high}	200	170	180	9.4	**20**
	CD45RA^{high}	760	40	300	57	**170**
OO5 (p17a/B35)	Total CD8	780	20	640	100	**640**
	CD45RO^{high}	1580	<10	1370	10	**140**
	CD45RA^{high}	160	10	140	70	**100**
O15 (p56/B7)	Total CD8	1010	30	2800	100	**2800**
	CD45RO^{high}	4510	30	6160	17	**1050**
	CD45RA^{high}	640	10	610	67	**410**
OO2 (p56/B7)	Total CD8	3500	10	3770	100	**3770**
	CD45RO^{high}	4610	150	4100	10	**410**
	CD45RA^{high}	980	10	760	53	**400**

[a] The contribution of CD45RA^{high} and CD45RO^{high} cells to the total pool of pp65 peptide-specific memory cells in PBMC was determined by multiplying the peptide-specific CTLp frequencies within each T cell subpopulation by the percentage of CD45RA^{high} or CD45RO^{high} cells within CD8$^+$ T cells in PBMC.
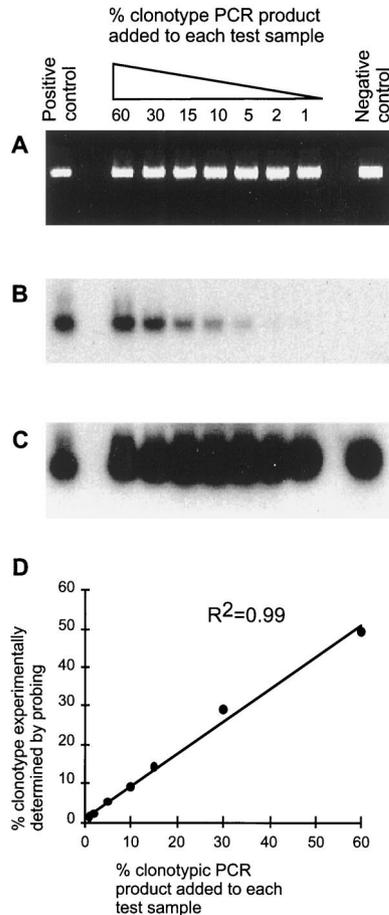
FIGURE 2. Determination of the accuracy and sensitivity of a TCR Vβ clonotyping technique. *A*, An increasing percentage of TCR Vβ PCR product from a pp65 peptide-specific CTL clone was added to TCR Vβ PCR product derived from pooled cDNA from four HCMV-seronegative donors; a sample of the clonal PCR product (positive control) and of the PCR product derived from the seronegative donors (negative control) was also included. *B*, After resolution on an agarose gel and transfer of the DNA to a nylon fiter, the filter was probed with a radiolabeled clonotypic probe. *C*, The filter was stripped of bound clonotypic probe and reprobed with a radiolabeled probe to the TCR C region. *D*, Percentage of clonotype derived by clonotypic probing technique plotted against percentage of clonotypic PCR product added to each test sample.

Massive expansion of CD45RO$^+$CD8$^+$ T cells, associated with fresh ex vivo pp65-specific cytotoxicity, during primary HCMV infection

The large clone sizes of pp65-specific memory CTL in CD45RA^{high}CD8$^+$ cells of long-term virus carriers suggest that following primary HCMV infection, some of the clonally expanded activated CD45RO^{high} pp65-specific CTL may have reverted to less activated memory CTL that reexpress the CD45RA^{high} phenotype. To address this possibility directly, we studied two patients during and after symptomatic primary HCMV infection.

Fresh PBMC were obtained from patient CMV104 at 3, 4, and 8 wk after the onset of symptoms (fever, anorexia, headache associated with atypical lymphocytosis, and abnormal liver function tests). PBMC were stained with anti-CD45RA, anti-CD45RO, and anti-CD8, and analyzed by flow cytometry (Fig. 4, *A*, *D*, *G*, *B*, *E*, and *H*); at each time point, PBL counts were determined in the clinical haematology laboratory, from which the absolute number of CD8$^+$ cells and the CD8$^+$CD45RA^{high} cells were calculated.

Aliquots of unstimulated PBMC were depleted of CD16$^+$ NK cells and used as effector cells in direct ex vivo cytotoxicity assays against HLA-matched target cells pulsed with the appropriate pp65 peptides (Fig. 4, *C*, *F*, and *I*). At 3 wk, there was a substantial CD8$^+$ lymphocytosis of 4.9 $\times$ 10^9/L (normal range of 0.4–1 $\times$ 10^9/L), the large majority of which were CD45RO^{high} (4.7 $\times$ 10^9/ L). At this time, there was a very high level of ex vivo cytotoxicity against two different HLA-B7-restricted pp65 peptides, p31 and p56. Similar results were obtained 1 wk later. At 8 wk after the onset of symptoms, the absolute CD8 count had decreased to 0.7 $\times$ 10^9 cells/L (within normal range) and there was a substantial reduction in the CD8$^+$CD45RO^{high} population. The absolute number of CD8$^+$CD45RA^{high} cells remained relatively stable at 3, 4, and 8 wk (0.2 $\times$ 10^9 cells/L, 0.5 $\times$ 10^9 cells/L, and 0.4 $\times$ 10^9 cells/L, respectivly). Thirty-eight weeks after onset of symptoms, CD8$^+$CD45RA^{high} cells were purified by negative sorting from PBMC and stimulated with autologous irradiated PBMC pulsed with peptide 56 in LDA. The frequency of peptide 56-specific CTLp in CD8$^+$CD45RA^{high} cells was 1240 per 10^6 CD8$^+$ T cells (frequency against control target <20 per 10^6 CD8$^+$CD45RA^{high} T cells).

A second patient (102) with primary HCMV infection was studied 3 wk after the onset of symptoms. At this time point, there was a large CD8$^+$ lymphocytosis, with a high percentage of these cells being CD45RO$^+$. There was also fresh ex vivo cytotoxicity against pp65 peptide-pulsed target cells. Eighteen weeks after onset of symptoms, PBMC obtained from patient 102 were sorted into total CD8, CD8$^+$CD45RA^{high}, and CD8$^+$CD45RO^{high} T cell populations, and the peptide-specific CTLp frequencies were determined for each population. Eighteen weeks after onset of symptoms, pp65 peptide-specific CTL were detected in both the CD45RA^{high}CD45RO$^-$ and CD45RO^{high}CD8$^+$ T cell subpopulations (data not shown).

Longitudinal analysis of pp65-specific clonotypes following primary HCMV infection shows clonal reversion from CD45RO^{high} to CD45RA^{high} T cells

Multiple independent pp65 peptide 56-specific CTL clones were derived from the PBMC of patient CMV104 4 wk after onset of symptoms, and the Vβ TCR usage of these clones was determined by PCR analysis with a panel of Vβ TCR primers, as described (16). A large proportion of the clones was found to utilize TCR Vβ 6.4. A clonotypic probe specific to the n-D-n region from one of these clones was used to quantitate the size of this pp65 peptide-specific CTL clone within the CD45RA^{high} and CD45RO^{high} CD8$^+$ T cell populations at 3, 4, 8, and 37 wk after onset of symptoms. The results show that at 3 wk after onset of symptoms, there was very little of the clonotype within the Vβ 6.4$^+$ CD45RA^{high} cell population as compared with the Vβ 6.4$^+$ CD45RO^{high} population (Fig. 5). Four weeks after onset of symptoms there was still a pronounced difference in the amount of clone detected in the CD45RA^{high} as compared with the CD45RO^{high} populations (Fig. 5). At 8 wk after onset, similar or higher levels of the clonotype were detected in the Vβ 6.4$^+$ CD45RA^{high} as compared with the Vβ 6.4$^+$ CD45RO^{high} population. At 37 wk after onset of symptoms, the clonotype was distributed in both the CD45RA^{high} and CD45RO^{high} T cell populations (Fig. 5), as seen previously in the long-term virus carriers (Table III, Fig. 3). As a mAb to TCR Vβ 6.4 is not commercially available, we were unable to calculate the absolute clone size within the CD45RA^{high} and CD45RO^{high} populations at each of the time points sampled.

Discussion

In CD8$^+$ PBMC of long-term HCMV carriers, we found that both the CD45RA^{high} and CD45RO^{high} populations contained HCMV

Table III. *Quantitation of pp65 peptide-specific clonotypes in total CD8$^+$ T cell populations and in the CD45RA^{high} and CD45RO^{high} CD8$^+$ subpopulations using clonotype probing*

Donor (peptide/class I restriction)	T Cell Population	Vβ Family	% of Vβ$^+$ Cells in CD8$^+$ PBMC by Flow Cytometry	Clonotype Sequence as a Percent of All TCR Vβ Sequences by Probing	Clone Size per 10^6 Cells in Each Population	Percent of Cells in CD8$^+$ PBMC by Flow Cytometry
OO1 (p69/A2)	Total CD8	13.1	9.8	74	72,500	100
	CD45RO^{high}		13.0	53	68,900	3.7
	CD45RA^{high}		7.0	61	42,700	74
OO9 (p56/B7)	Total CD8	14	3.6	18	6,480	100
	CD45RO^{high}		9.8	2	1,960	9.4
	CD45RA^{high}		3.5	10	3,500	57
OO5 (p17a/B35)	Total CD8	20	20.0	15	30,000	100
	CD45RO^{high}		1.0	28	2,800	10
	CD45RA^{high}		17.0	4	6,800	70
O15 (p56/B7)	Total CD8	6.4	NA	28	NA^b	100
	CD45RO^{high}		NA	14	NA	17
	CD45RA^{high}		NA	7	NA	67
OO2 (p56/B7)	Total CD8	14	13.0	64	83,200	100
	CD45RO^{high}		12.6	50	63,000	10
	CD45RA^{high}		14.0	54	75,600	53

[a] The contribution of CD45RA^{high} and CD45RO^{high} cells to the total pool of pp65 peptide-specific clonotype in PBMC was determined by multiplying the clone size within each T cell subpopulation by the percentage of CD45RA^{high} or CD45RO^{high} cells within CD8$^+$ T cells in PBMC.

[b] NA, mAb to TCR Vβ 6.4 is not available.

pp65 peptide-specific CTLp; many of the peptide-specific memory CTL in PBMC were CD45RA^{high}. We found that an individual CTL clonotype could be distributed in both the CD45RA^{high} and CD45RO^{high} populations, and in some cases was more abundant in the CD45RA^{high} population. During primary HCMV infection, we observed fresh ex vivo pp65 peptide-specific cytotoxicity associated with a large increase in CD45RO$^+$CD8$^+$ T cells in PBMC. At

FIGURE 3. Quantitation of an individual peptide 56-specific clone within the total CD8$^+$ population and the CD45RA^{high} and CD45RO^{high} subpopulations of donor 002. *A*, Duplicate TCR Vβ PCR products were derived from each of the T cell populations; PCR product derived from the biological peptide 56-specific CTL clone (positive control) and PCR product derived from pooled cDNA from PBMC of four HCMV-seronegative donors (negative control) were resolved on a 1.5% agarose gel, transferred to a filter, and probed with a radiolabeled clonotypic probe. *B*, The filter was stripped of bound clonotypic probe and reprobed with a radiolabeled probe to the TCR C region. The binding of the probes was quantitated using a phosphor imager, and for each population the clonotype sequence as a percentage of all TCR Vβ sequences was calculated according to the formula in *Materials and Methods*. Clonotypic analysis for all donors is shown in Table III.

subsequent time points, both the CD45RA^{high} and CD45RO^{high} populations contained peptide-specific CTLp, and a virus-specific CTL clone that was initially CD45RO^{high} was subsequently distributed in both the CD45RO^{high} and the CD45RA^{high} populations.

Previous studies of the human CD8$^+$ CTL response against another persistent virus, EBV, reported substantially higher CTLp frequencies in the CD45RO^{high} population (110–355 per 10^6 CD45RO^{high} cells) compared with the CD45RA^{high} population (3–27 per 10^6 CD45RA^{high} cells) (6). In most healthy HCMV carriers, we also observed higher HCMV-specific CTLp frequencies in CD45RO^{high} cells (200–4610 per 10^6 CD45RO^{high}CD8$^+$ T cells) compared with the CD45RA^{high} population (160–980 per 10^6 CD45RA^{high}CD8$^+$ T cells). However, the absolute frequencies of pp65-specific CTLp that we observed in the CD45RA^{high} population were 5–35-fold higher than previously observed for EBV-specific CTLp in the CD45RA^{high} population. Because it is impossible to purify intermediate CD45RA$^+$RO$^+$ by negative selection, we were not able to determine directly the contribution of intermediate CD45RA$^+$RO$^+$ cells. Thus, the sum of the calculated frequencies of CTLp in the CD45RO^{high} and CD45RA^{high} fall short of the total CD8$^+$ frequencies; this is probably due to contributions from the RO$^+$RA$^+$ subset that are not assayed in this study. The higher frequencies in our experiments may reflect improved cloning efficiency due to the addition of exogenous IL-2 and the longer period of LDA culture that we used before cytotoxicity assay (14 days, compared with 7–9 days in Ref. 6). Following stimulation, the initial rate of proliferation of CD45RO^{high} cells is greater than that of CD45RA^{high} cells (4). Therefore, with a longer period of culture in the presence of IL-2, CTLp within the CD45RA^{high} population had sufficient time to grow into detectable CTL clones in vitro, leading to substantially higher estimates of CTLp frequency in the CD45RA^{high} population. Because there are many more CD45RA^{high}CD8$^+$ T cells than CD45RO^{high}CD8$^+$ T cells in PBMC, in absolute terms up to 10-fold more of the HCMV-specific CTLp in PBMC are in the CD45RA^{high} population.

The size of individual peptide-specific CTL clonotypes determined by clonotype probing was 10–100-fold larger than the corresponding peptide-specific CTLp frequency determined by LDA
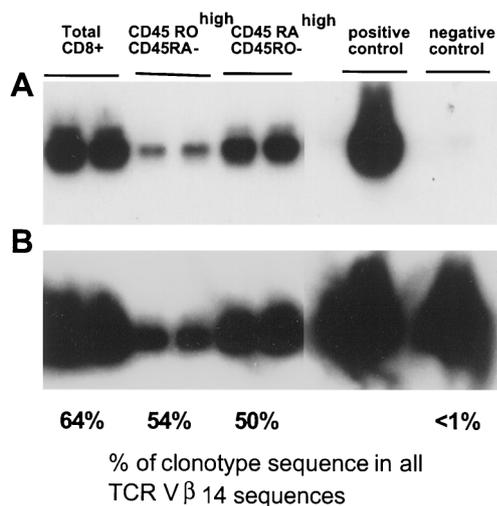
FIGURE 4. CD45RO and RA expression on CD8$^+$ T cells and fresh ex vivo peptide-specific cytotoxicity in primary HCMV infection in donor 104. *A, D,* and *G,* The percentage of CD8$^+$ T cells in fresh PBMC at 3, 4, and 8 wk after onset of symptoms. *B, E,* and *H,* The distribution of CD45RA and CD45RO on CD8$^+$ T cells in fresh PBMC. *C, F,* and *I,* Fresh ex vivo cytotoxicity in PBMC at an E:T ratio of 40:1 against autologous target cells pulsed with pp65 peptides 69, 31, and 56, and unpulsed.
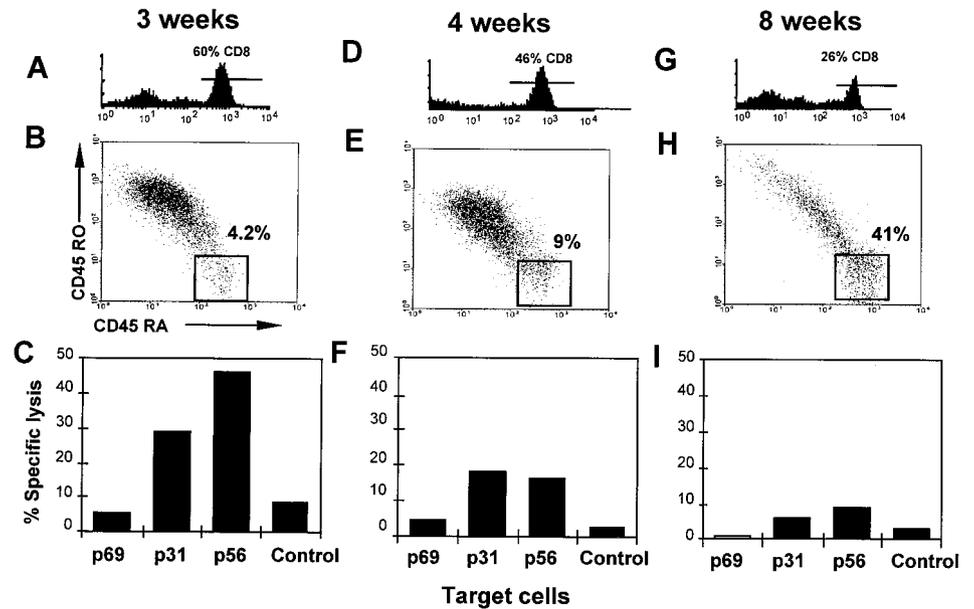
(which represents the aggregate functional response of all of the CTL clonotypes specific to the same peptide) in the same blood sample. Clonotype probing is sufficiently sensitive to detect individual clonotype sequences that constitute as little as 1% of sequences in a Vβ family, and hence about 0.1% of CD8$^+$ cells in PBMC, because unlike LDA clonotype detection, it does not involve biological cloning. Staining with fluorescent peptide-MHC class I tetramers (18) also provides greater sensitivity than LDA for detecting the aggregate of peptide-specific CTL clones that can bind to a given peptide-MHC (19). In this study, we used clonotype probing rather than tetramer staining not only because we wished to study memory CTL responses specific for different viral peptides restricted by three different MHC alleles, but also because the clonotype probing technique provides a higher level of resolution by allowing the study of reversion from CD45RO^{high} to CD45RA^{high} at the level of an individual CTL clone.

In response to acute virus infections, there are large expansions of virus-specific CD8$^+$ T cells (10, 19, 20). Highly activated hu-

man CD45RO$^+$CD8$^+$ T cells show increased susceptibility to apoptosis, but the survival of these activated CD8$^+$ cells in vitro can be prolonged by provision of help from nonlymphoid cells (21, 22). Human CD45RO^{high} cells appear to turn over more rapidly than CD45RA^{high} cells in vivo, with indirect evidence that CD45RO^{high} T cells may revert to CD45RA^{high} cells in vivo (8). Our finding of large clone sizes of the same pp65-specific CTL clonotype in both the CD45RO^{high} and the CD45RA^{high} CD8$^+$ cells of long-term virus carriers suggested that after primary HCMV infection, some of the clonally expanded activated CD45RO^{high} pp65-specific CTL reverted to (less activated) memory CTL that reexpress the CD45RA^{high} phenotype. Our observations in primary HCMV infection provide direct evidence that cells of defined virus-specific CTL clonotypes revert from CD45RO^{high} to CD45RA^{high} in vivo.

The relative distribution of memory CD8$^+$ T cells between the CD45RO^{high} and CD45RA^{high} populations may be influenced by the degree to which these cells are exposed to Ag in vivo. HCMV
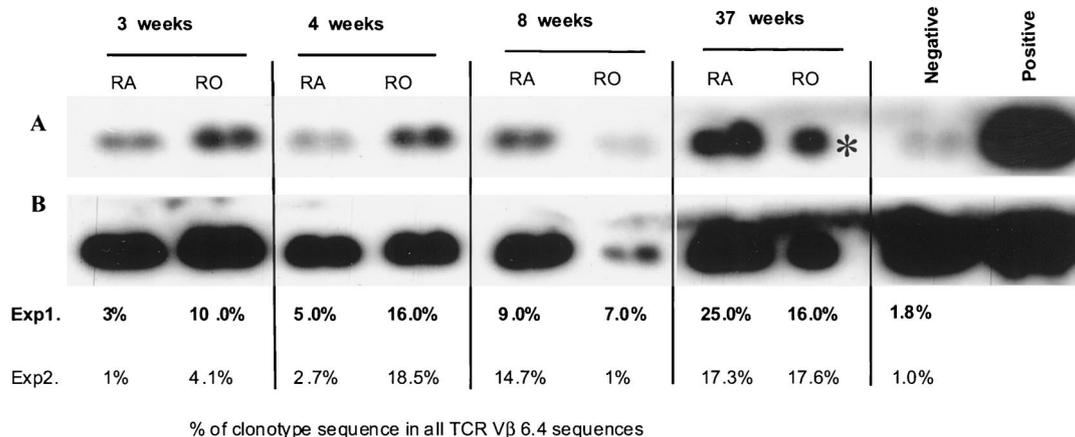

% of clonotype sequence in all TCR Vβ 6.4 sequences

FIGURE 5. Quantitation of an individual peptide 56-specific clone within CD45RA^{high} and CD45RO^{high} CD8$^+$ T cell subpopulations derived from PBMC of donor 104 during and after primary HCMV infection. *A,* Duplicate TCR Vβ 6.4 PCR products were amplified from each of the T cell populations taken at 3, 4, 8, and 37 wk after onset of symptoms. PCR product derived from the biological pp65-specific clone (positive control) and pooled PCR product derived from PBMC of four HCMV-seronegative donors (negative control) were probed with a radiolabeled clonotypic probe. *B,* The filter was stripped of bound clonotypic probe and reprobed with a radiolabeled probe specific to the TCR C region. For each subpopulation, the clonotype sequence as a percentage of all TCR Vβ 6.4$^+$ sequences is shown for two independent amplifications and probing experiments; % in bold represents the gel shown. *, Duplicate PCR sample failed.

persists in cells of the myeloid lineage (11, 12) from which infectious virus can reactivate (23). Productive HCMV infection is rare in most body compartments in healthy subjects, and HCMV DNA cannot be detected in normal plasma by highly sensitive PCR (11, 12). At least for this persistent human virus infection, memory CD8$^+$ T cells are a phenotypically heterogenous population of clonally expanded cells; some are CD45RO^{high} cells that as a population are more activated and may turn over more rapidly (8), while others that are CD45RA^{high} are less activated and divide infrequently. This is consistent with in vivo studies of murine models, in which phenotypic markers of activation are not identical to those in humans (24). Using adoptive transfer of CD8$^+$ T cells from transgenic mice expressing an LCMV peptide-specific TCR, Zimmermann et al. (25) were able to visualize memory T cells by flow cytometry following LCMV infection in vivo. They observed heterogeneity both in cell surface expression of memory markers (most CD8$^+$ memory T cells were CD11b$^-$ and CD45RB^{high}, like naive mouse T cells) and in intermitotic interval (one-half of the transgenic memory T cells persisted for 5–7 wk without undergoing cell division). Following acute infection in intact mice, virus-specific memory CTL responses can be maintained at a stable level for many months (26, 27). These CD8$^+$ T cell responses can nevertheless be modulated by subsequent infections with different viruses. In response to virus infection in mice, most of the activated CD44^{high}CD8$^+$ T cells undergo cell division; this preferential proliferation of CD44^{high}CD8$^+$ T cells can be mimicked by type I IFN (28). Once the immune system returns to homeostasis following infection with a different virus, the CTL memory pool to earlier viruses diminishes (27). The clonal composition differs between primary and memory T cell responses in some murine models, but not others (29, 30). Because the clonotype probing technique we describe is able to distinguish individual CTL clones, we are currently using this technique to determine whether the clonal composition of the virus-specific CTL response changes with time following primary infection.

The extent to which CD4$^+$ T cells may undergo interconversion between CD45RA^{high} and CD45RO^{high} either in vitro or in vivo is much debated (31). Recent evidence that human memory CD4$^+$ T cell responses are confined to the CD45RO^{high} population (32) suggests that, at least in humans, the capacity of memory CD8$^+$ T cells to reexpress CD45RA^{high} in vivo may genuinely be different from that of CD4$^+$ T cells.

We have shown that cells of defined virus-specific CD8$^+$ CTL clonotypes revert from CD45RO^{high} to CD45RA^{high} in vivo. Because CD45RA^{high} cells contain both naive cells and memory cells, we conclude that CD45RA is not a reliable marker of naivety in human CD8$^+$ T cells and that CD45RO is a marker of cell activation that does not identify all CD8$^+$ memory T cells.

References

1. Janeway, C. A. Jr. 1992. The T cell receptor as a multicomponent signalling machine: CD4/CD8 coreceptors and CD45 in T cell activation. *Annu. Rev. Immunol. 10:645.*
2. Prince, H. E., J. York, and E. R. Jensen. 1992. Phenotypic comparison of the three populations of human lymphocytes defined by CD45RO and CD45RA expression. *Cell. Immunol. 145:254.*
3. Zola, H., L. Flego, P. J. Macardle, P. J. Donohoe, J. Ranford, and D. Roberton. 1992. The CD45RO (p180, UCHL1) marker: complexity of expression in peripheral blood. *Cell. Immunol. 145:175.*
4. De Jong, R., M. Brouwer, F. Miedema, and R. A. van Lier. 1991. Human CD8$^+$ T lymphocytes can be divided into CD45RA$^+$ and CD45RO$^+$ cells with different requirements for activation and differentiation. *J. Immunol. 146:2088.*
5. Okumura, M., Y. Fujii, K. Inada, K. Nakahara, and H. Matsuda. 1993. Both CD45RA$^+$ and CD45RA$^-$ subpopulations of CD8$^+$ T cells contain cells with high levels of lymphocyte function-associated antigen-1 expression, a phenotype of primed T cells. *J. Immunol. 150:429.*

6. Merkenschlager, M., and P. C. Beverley. 1989. Evidence for differential expression of CD45 isoforms by precursors for memory-dependent and independent cytotoxic responses: human CD8 memory CTLp selectively express CD45RO (UCHL1). *Int. Immunol. 1:450.*
7. Dutton, R. W., L. M. Bradley, and S. L. Swain. 1998. T cell memory. *Annu. Rev. Immunol. 16:201.*
8. Michie, C. A., A. McLean, C. Alcock, and P. C. Beverley. 1992. Lifespan of human lymphocyte subsets defined by CD45 isoforms. *Nature 360:264.*
9. Fujii, Y., M. Okumura, K. Inada, and K. Nakahara. 1992. Reversal of CD45R isoform switching in CD8$^+$ T cells. *Cell. Immunol. 139:176.*
10. Callan, M. F., L. Tan, N. Annels, G. S. Ogg, J. D. Wilson, C. A. O'Callaghan, N. Steven, A. J. McMichael, and A. B. Rickinson. 1998. Direct visualization of antigen-specific CD8$^+$ T cells during the primary immune response to Epstein-Barr virus in vivo. *J. Exp. Med. 187:1395.*
11. Taylor Wiedeman, J., P. Sissons, and J. Sinclair. 1994. Induction of endogenous human cytomegalovirus gene expression after differentiation of monocytes from healthy carriers. *J. Virol. 68:1597.*
12. Mendelson, M., S. Monard, P. Sissons, and J. Sinclair. 1996. Detection of endogenous human cytomegalovirus in CD34$^+$ bone marrow progenitors. *J. Gen. Virol. 77:3099.*
13. Borysiewicz, L. K., J. K. Hickling, S. Graham, J. Sinclair, M. P. Cranage, G. L. Smith, and J. G. Sissons. 1988. Human cytomegalovirus-specific cytotoxic T cells: relative frequency of stage-specific CTL recognizing the 72-kD immediate early protein and glycoprotein B expressed by recombinant vaccinia viruses. *J. Exp. Med. 168:919.*
14. Reusser, P., S. R. Riddell, J. D. Meyers, and P. D. Greenberg. 1991. Cytotoxic T-lymphocyte response to cytomegalovirus after human allogeneic bone marrow transplantation: pattern of recovery and correlation with cytomegalovirus infection and disease. *Blood 78:1373.*
15. McLaughlin Taylor, E., H. Pande, S. J. Forman, B. Tanamachi, C. R. Li, J. A. Zaia, P. D. Greenberg, and S. R. Riddell. 1994. Identification of the major late human cytomegalovirus matrix protein pp65 as a target antigen for CD8$^+$ virus-specific cytotoxic T lymphocytes. *J. Med. Virol. 43:103.*
16. Wills, M. R., A. J. Carmichael, K. Mynard, X. Jin, M. P. Weekes, B. Plachter, and J. G. Sissons. 1996. The human cytotoxic T-lymphocyte (CTL) response to cytomegalovirus is dominated by structural protein pp65: frequency, specificity, and T-cell receptor usage of pp65-specific CTL. *J. Virol. 70:7569.*
17. Weekes, M. P., M. R. Wills, K. Mynard, A. J. Carmichael, and J. G. Sissons. 1999. The memory cytotoxic T-lymphocyte (CTL) response to human cytomegalovirus infection contains individual peptide-specific CTL clones that have undergone extensive expansion in vivo. *J. Virol. 73:2099.*
18. Altman, J. D., P. A. H. Moss, P. J. R. Goulder, D. H. Barouch, M. G. McHeyzer Williams, J. I. Bell, A. J. McMichael, and M. M. Davis. 1996. Phenotypic analysis of antigen-specific T lymphocytes. *Science 274:94.*
19. Murali Krishna, K., J. D. Altman, M. Suresh, D. J. Sourdive, A. J. Zajac, J. D. Miller, J. Slansky, and R. Ahmed. 1998. Counting antigen-specific CD8 T cells: a reevaluation of bystander activation during viral infection. *Immunity 8:177.*
20. Ahmed, R., and D. Gray. 1996. Immunological memory and protective immunity: understanding their relation. *Science 272:54.*
21. Akbar, A. N., N. Borthwick, M. Salmon, W. Gombert, M. Bofill, N. Shamsadeen, D. Pilling, S. Pett, J. E. Grundy, and G. Janossy. 1993. The significance of low *bcl*-2 expression by CD45RO T cells in normal individuals and patients with acute viral infections: the role of apoptosis in T cell memory. *J. Exp. Med. 178:427.*
22. Gombert, W., N. J. Borthwick, D. L. Wallace, H. Hyde, M. Bofill, D. Pilling, P. C. Beverley, G. Janossy, M. Salmon, and A. N. Akbar. 1996. Fibroblasts prevent apoptosis of IL-2-deprived T cells without inducing proliferation: a selective effect on Bcl-X$_L$ expression. *Immunology 89:397.*
23. Soderberg Naucler, C., K. N. Fish, and J. A. Nelson. 1997. Reactivation of latent human cytomegalovirus by allogeneic stimulation of blood cells from healthy donors. *Cell 91:119.*
24. Tanchot, C., F. A. Lemonnier, B. Perarnau, A. A. Freitas, and B. Rocha. 1997. Differential requirements for survival and proliferation of CD8 naive or memory T cells. *Science 276:2057.*
25. Zimmerman, C., K. Brduscha Riem, C. Blaser, R. M. Zinkernagel, and H. Pircher. 1996. Visualization, characterization, and turnover of CD8$^+$ memory T cells in virus-infected hosts. *J. Exp. Med. 183:1367.*
26. Lau, L. L., B. D. Jamieson, T. Somasundaram, and R. Ahmed. 1994. Cytotoxic T-cell memory without antigen. *Nature 369:648.*
27. Selin, L. K., K. Vergilis, R. M. Welsh, and S. R. Nahill. 1996. Reduction of otherwise remarkably stable virus-specific cytotoxic T lymphocyte memory by heterologous viral infections. *J. Exp. Med. 183:2489.*
28. Tough, D. F., P. Borrow, and J. Sprent. 1996. Induction of bystander T cell proliferation by viruses and type I interferon in vivo. *Science 272:1947.*
29. McHeyzer Williams, M. G., and M. M. Davis. 1995. Antigen-specific development of primary and memory T cells in vivo. *Science 268:106.*
30. Maryanski, J. L., C. V. Jongeneel, P. Bucher, J. L. Casanova, and P. R. Walker. 1996. Single-cell PCR analysis of TCR repertoires selected by antigen in vivo: a high magnitude CD8 response is comprised of very few clones. *Immunity 4:47.*
31. Bell, E. B., S. M. Sparshott, and C. Bunce. 1998. CD4$^+$ T-cell memory, CD45R subsets and the persistence of antigen: a unifying concept. *Immunol. Today 19:60.*
32. Young, J. L., J. M. Ramage, J. S. Gaston, and P. C. Beverley. 1997. In vitro responses of human CD45R0^{bright}RA$^-$ and CD45R0$^-$RA^{bright} T cell subsets and their relationship to memory and naive T cells. *Eur. J. Immunol. 27:2383.*